Impact of Optical Properties on the Controllability of Solar Sails

Alesia Herasimenka, Lamberto Dell'Elce, Jean-Baptiste Caillau, Jean-Baptiste Pomet

IMPACT OF OPTICAL PROPERTIES ON THE CONTROLLABILITY OF SOLAR SAILS

A. Herasimenka[(1)(3)], L. Dell'Elce[(2)], J.-B. Caillau[(1)], J.-B. Pomet[(2)]

[(1)] *Université Côte d'Azur, CNRS, Inria, LJAD, Nice, France*
[(2)] *Inria, Sophia Antipolis, France*
[(3)] *alesia.herasimenka@univ-cotedazur.fr*

ABSTRACT

This manuscript is devoted to the analysis of the local controllability of non-ideal solar sails in planet-centered orbits. Classical approaches fail when considering this control problem because sails cannot generate forces with positive components toward the Sun direction. More precisely, the control set is delimited by a convex cone of revolution with axis toward the Sun and, as such, it is not defined in a neighborhood of the origin, which precludes the use of standard sufficient conditions for controllability. A novel necessary condition is introduced that certifies the non-controllability of the system for given optical properties of the sail and orbital elements. The condition can be verified by solving a semi-infinite programming problem. Numerical solution is achieved by leveraging on the formalism of squared functional systems. Minimal optical requirements of the sail are inferred for all combinations of orbital elements. These results are independent of the planetary constant.

1 INTRODUCTION

Solar sails offer a propellant-less solution to achieve interplanetary transfers, planet escapes, and de-orbiting maneuvers by leveraging on solar radiation pressure (SRP) [1]. Although very few solar sail missions were launched, the possibility to use SRP as an inexhaustible source of propulsion attracted the interest of researchers since decades, and several contributions on the guidance and control of solar sails are available. Specifically, a large body of literature focuses on the mathematical formulation and numerical solution of optimal transfers (mostly minimum time) and locally optimal maneuvers, i.e., maximization of the instantaneous rate of change of a desired orbital element. Most often, solutions of two-point boundary value problems are offered without investigating whether the targeted point is within the reachable set of the control system, which, admittedly, is a challenging task at best. We believe that the true effort in finding feasible solutions to the transfer of solar sails is mostly hidden because, in layman's terms, only satisfactory solutions are published. Surprisingly enough, a thorough analysis of the controllability of solar sails is not available to date.

A major difficulty in assessing the controllability of an SRP-actuated system is that the sail cannot generate a force with a positive component toward the direction of the Sun, so that classical tools of geometric control theory cannot be used. For example, Lie algebra of the system is full rank (unless a fully absorptive model of the sail is considered), but this result, which should indicate that the system is weakly controllable, requires that the interior of the control set includes the origin, *i.e.*, both positive and negative controls should be generated, so that it is not sufficient to analyze the sailing problem. This aspect is particularly critical when considering a non-ideal sail (by ideal, we mean a perfectly

reflective flat surface) because the control set is contained inside a strictly convex cone of revolution, whose angle depends on the optical properties of the sail.

In this context, a necessary condition is proposed for the local controllability of non-ideal solar sails in planet-centered orbit (e.g., escape trajectory). This requirement is aimed at assessing whether the sail at hand is capable of decreasing all possible functions of the Keplerian integrals of motion over an orbital period. The necessary condition is formulated as a worst-case optimization problem characterized by a finite number of design variables and a two-parameter family of inequality constraints, namely, the clock angle of the convex cone and the true anomaly of the sail. This formulation relies on the convexification of the control set for different optical coefficients by defining the minimal cone containing all possible directions of the force vector. Numerical solution of this semi-infinite programming problem is achieved by replacing the cone of revolution with a polyhedral one, and by leveraging on the formalism of squared functional system to exactly enforce inequality constraints for all values of the true anomaly. Eventually, the semi-infinite problem is recast into a finite-dimensional convex programming with a finite number of linear matrix inequalities (LMI) and an unique well-defined solution.

An exhaustive analysis covering the entire phase space of orbital elements is offered (specifically, all shape, size and orientation of the orbital plane). A minimum angle is found for any combination of orbital elements, which satisfies the necessary condition. This result is planet-independent. The methodology is unaware of the specific source of non-ideality of the sail (e.g., specular or diffuse reflection, re-emitted radiation [2]) since it only uses the conical hull of the control set. This result can be used to provide insight into the controllability of the sail during its lifetime, owing to the degradation of its surface discussed in [3], and may support the design of real-life missions by serving as a minimal requirement to be satisfied. The case of heliocentric orbits is also briefly discussed.

2 SOLAR SAILS DYNAMICS

2.1 Force model

Solar sails use solar radiation pressure (SRP) as a propulsive means to control their trajectory. SRP is due to the interaction between photons and surface of the sail. The magnitude of the pressure depends on the Sun-sail distance, $r_\odot$. Specifically, denoting by $\Phi_{SR} \approx 1367$ W m^{-2} the solar flux at 1 AU and by c the speed of light, a simple model is [4, Chap. 3]:

$$P = \frac{\Phi_{SR}}{c\, r_\odot^2}$$

A flat sail with surface A and mass m is considered in this work. The resulting force depends on various optical and geometrical properties of the sail and it is obtained by summing up contributions of the incoming, reflected, and thermal radiations, namely $\boldsymbol{f}_a$, $\boldsymbol{f}_r$, and $\boldsymbol{f}_e$. In addition, the reflected force is divided into specular and diffuse components, $\boldsymbol{f}_{rs}$ and $\boldsymbol{f}_{ru}$, respectively. The first one is caused by photons that are reflected symmetrically with respect to the normal of the sail and create moment in the opposite direction. Conversely, diffuse reflection results form surface roughness, which causes photons to be uniformly reflected in all directions, yielding a component of the force toward the vector normal to the sail. Finally, absorbed photons are then re-radiated in all directions with energy dependent on the temperature of the sail, generating another component of the force that is normal to its surface. Figure 1a shows the directions of the various components. Denoting by $\hat{\boldsymbol{s}}$ the direction of the Sun, $\hat{\boldsymbol{n}}$ the unit vector normal to the sail with positive projection toward $\hat{\boldsymbol{s}}$, i.e., $\cos\beta = \hat{\boldsymbol{n}} \cdot \hat{\boldsymbol{s}} \geq 0$, and

$$\hat{\boldsymbol{t}} = \frac{\hat{\boldsymbol{n}} \times \hat{\boldsymbol{s}}}{\|\hat{\boldsymbol{n}} \times \hat{\boldsymbol{s}}\|} \times \hat{\boldsymbol{n}} = \frac{\hat{\boldsymbol{s}} - \cos\beta\, \hat{\boldsymbol{n}}}{\sin\beta}$$

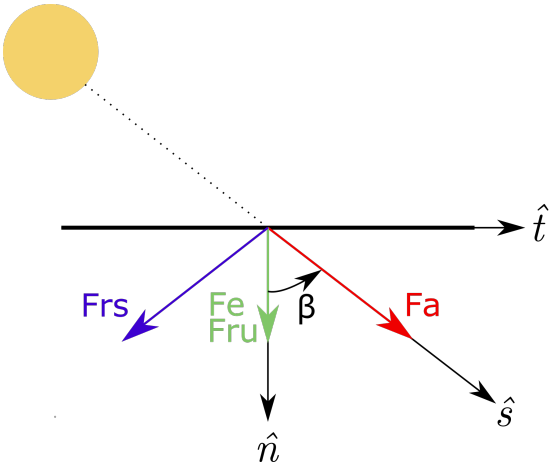

(a) Schematic representation.

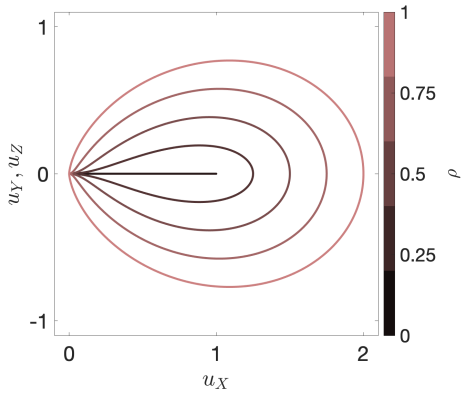

(b) Control sets for different reflectivity coefficients and $s = 1$. Here, u_X is the projection of $\boldsymbol{u}$ toward $\hat{\boldsymbol{s}}$, while u_Y and u_Z are orthogonal components.

Figure 1: Components of the SRP force.

the tangent unit vector in the plane generated by $\hat{\boldsymbol{s}}$ and $\hat{\boldsymbol{n}}$, the components of the specific force are [2]

$$\begin{aligned}
\boldsymbol{f}_a &= \varepsilon(r_\odot)\cos\beta(\cos\beta\,\hat{\boldsymbol{n}} + \sin\beta\,\hat{\boldsymbol{t}}) \\
\boldsymbol{f}_{rs} &= \varepsilon(r_\odot)\rho s\cos\beta(\cos\beta\,\hat{\boldsymbol{n}} - \sin\beta\,\hat{\boldsymbol{t}}) \\
\boldsymbol{f}_{ru} &= \varepsilon(r_\odot)B_f\rho(1-s)\cos\beta\,\hat{\boldsymbol{n}} \\
\boldsymbol{f}_e &= \varepsilon(r_\odot)(1-\rho)\frac{\varepsilon_f B_f - \varepsilon_b B_b}{\varepsilon_b + \varepsilon_f}\cos\beta\,\hat{\boldsymbol{n}}
\end{aligned} \tag{1}$$

where the function $\varepsilon(r_\odot) = APm^{-1}$ has small magnitude, $\rho \in [0,1]$ is the portion of reflected radiation, $s \in [0,1]$ the fraction of specular reflection, and ε_b, ε_f, B_b, B_f back and front surface emissivity and Lambertian coefficients respectively. The resulting force is thus

$$\boldsymbol{f}_{SRP} = \boldsymbol{f}_a + \boldsymbol{f}_{rs} + \boldsymbol{f}_{ru} + \boldsymbol{f}_e$$

Sails use $\boldsymbol{f}_{SRP}$ as thrust force. In the reminder of the paper, control variable is $\boldsymbol{u} = \dfrac{\boldsymbol{f}_{SRP}}{\varepsilon(r_\odot)}$. Control set is:

$$\mathcal{U} = \left\{ \frac{\boldsymbol{f}_{SRP}(\hat{\boldsymbol{n}})}{\varepsilon(r_\odot)},\ \hat{\boldsymbol{n}} \in \mathbb{R}^3,\ \|\hat{\boldsymbol{n}}\| = 1 \right\}$$

Figure 1b shows the control set for various optical properties. We note that the set is not convex. Re-emitted component is generally negligible when compared to other contributions. Two extreme cases can be identified: ideal sails are constituted by perfectly reflective surfaces ($\rho = s = 1$), whereas perfectly-absorptive surfaces are a worst-case scenario ($\rho = 0$, $\boldsymbol{f}_e$ neglected). In fact, the control set of a perfect sail includes all possible sets obtained with non-ideal parameters. Although sails are designed to be as ideal as possible, optical properties degrade with time. Hence, the fraction of reflected radiation decreases with life time of the satellite, as discussed in [3].

2.2 Equations of motion

We study the motion of a solar sail around a planet. The objective of this work is to infer whether geometric constraints of the control set (which are function of the optical properties of the sail as

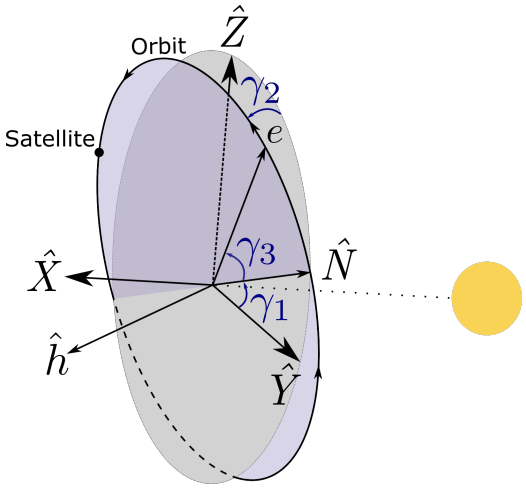

Figure 2: Euler angles orienting the orbit with respect to the reference frame. Here, $\boldsymbol{h}$ and $\boldsymbol{e}$ denote the angular momentum and eccentricity vectors.

discussed in Section 2.1) prevent the sail from arbitrarily modifying its orbit. To this purpose, we neglect all perturbations but SRP, and the motion of the sail is modeled as

$$\frac{\mathrm{d}^2\boldsymbol{r}}{\mathrm{d}\,t^2} = -\frac{\mu}{r^3}\boldsymbol{r} + \varepsilon(r_\odot)\boldsymbol{u} \tag{2}$$

where μ and $\boldsymbol{r}$ denote the gravitational constant of the planet and position vector, respectively. Compensating the drift of a specific perturbation concerns the sizing of the sail and it is beyond the scope of the paper.

We assume that orbital period of the sail is much smaller than the one of the heliocentric orbit of the planet, so that variations of the Sun direction $\hat{\boldsymbol{s}}$ over a single period are neglected. In addition, eclipses are also ignored, which yields results that are both independent of the radius of the planet and conservative (in the sense that the proposed methodology guarantees non controllability of System 2).

Consider a pseudo-inertial reference frame with origin at the center of the planet, $\hat{\boldsymbol{X}}$ axis aligned to $\hat{\boldsymbol{s}}$, $\hat{\boldsymbol{Y}}$ toward an arbitrary orthogonal direction, and $\hat{\boldsymbol{Z}}$ completes the right-hand frame. Let γ_1, γ_2, γ_3 be Euler angles orienting the eccentricity vector according to a $X-Y-X$ rotation as depicted in Fig. 2, and a, e, and f be the semi-major axis and eccentricity and true anomaly, respectively. The specific choice of Euler angles follows from the symmetry of System (2), *i.e.* (all results will be independent of γ_1). Motion of slow elements, $I = (\gamma_1, \gamma_2, \gamma_3, a, e)^T$, is governed by

$$\frac{\mathrm{d}\,I}{\mathrm{d}\,t} = \varepsilon(r_\odot)\sqrt{\frac{a\,(1-e^2)}{\mu}}G(I,f)\,R(I,f)\,\boldsymbol{u} \tag{3}$$

where components of $\boldsymbol{u}$ are in the reference frame, $R = R_X(\gamma_3 + f)R_Y(\gamma_2)R_X(\gamma_1)$ is the rotation matrix from reference to local-vertical local-horizontal frames[1], and $G(I,f)$ can be deduced from

[1]Here, $R_A(\varphi)$ denotes the rotation matrix of angle φ about the axis $\hat{\boldsymbol{A}}$.

Gauss variational equations (GVE) of classical elements:

$$G = \begin{pmatrix} 0 & 0 & \dfrac{\sin(\gamma_3+f)}{\sin\gamma_2(1+e\cos f)} \\ 0 & 0 & \dfrac{\cos(\gamma_3+f)}{1+e\cos f} \\ -\dfrac{\cos f}{e} & \dfrac{2+e\cos f}{1+e\cos f}\dfrac{\sin f}{e} & \dfrac{\cos(\gamma_3+f)}{1+e\cos f} \\ \dfrac{2\,a\,e}{1-e^2}\sin f & \dfrac{2\,a\,e}{1-e^2}(1+e\cos f) & 0 \\ \sin f & \dfrac{e\cos^2 f+2\cos f+e}{1+e\cos f} & 0 \end{pmatrix}$$

We note that $(1+e\cos f)\,G(I,f)R(I,f)$ is trigonometric in f. This consideration offers significant advantages to the numerical methodology detailed in Section 4.2.

3 CLASSICAL APPROACH TO LOCAL CONTROLLABILITY

Local controllability of control-affine systems is guaranteed if the following conditions are verified [5, Chap. 4]:

i The drift, *i.e.*, non-controlled motion, is periodic or recurrent;

ii Vector fields are bracket generating, namely Lie algebra of the system is full rank;

iii The convex hull of the control set $\mathcal{U}$ is a neighbourhood of the origin in $\mathbb{R}^m$.

Drift of Eq. (2) is Keplerian, which is periodic for elliptic orbits. As such, the first condition is verified for the problem at hand.

Concerning the rank of Lie algebra, two different scenarios have to be analyzed. The first one concerns *perfectly-absorptive sails*. Here, $\boldsymbol{u} = \hat{\boldsymbol{s}}u$, so that the control set degenerates to a segment aligned to $\hat{\boldsymbol{s}}$, as shown in Fig. 1b (for $\rho = 0$). Appendix A offers a detailed evaluation of Lie brackets in this case, which shows that the algebra is rank deficient. This allows to conclude the non-controllability of the system. Moreover, rank deficiency suggests that an integral of motion exists, which happens to be the projection of the angular momentum $\boldsymbol{h}$ toward $\hat{\boldsymbol{s}}$, namely $\hat{\boldsymbol{s}}\cdot\boldsymbol{h} = \hat{\boldsymbol{s}}\cdot(\boldsymbol{r}\times\boldsymbol{v}) = \det(\boldsymbol{r},\boldsymbol{v},\hat{\boldsymbol{s}})$, where $\boldsymbol{v}$ is the velocity vector. In fact, Lie derivative of $\hat{\boldsymbol{s}}\cdot\boldsymbol{h}$ with respect to the controlled vector field, $F^1 = s_X\frac{\partial}{\partial v_X} + s_Y\frac{\partial}{\partial v_Y} + s_Z\frac{\partial}{\partial v_Z}$ is:

$$\begin{aligned} L_{F^1}(\det(\boldsymbol{r},\boldsymbol{v},\hat{\boldsymbol{s}})) &= s_X\frac{\partial}{\partial v_X}\det(\boldsymbol{r},\boldsymbol{v},\hat{\boldsymbol{s}}) + s_Y\frac{\partial}{\partial v_Y}\det(\boldsymbol{r},\boldsymbol{v},\hat{\boldsymbol{s}}) + s_Z\frac{\partial}{\partial v_Z}\det(\boldsymbol{r},\boldsymbol{v},\hat{\boldsymbol{s}}) \\ &= s_X(-r_Y s_Z + r_Z s_Y) + s_Y(r_X s_Z - r_Z s_X) + s_Z(-r_X s_Y + r_Y s_X) \\ &= 0 \end{aligned}$$

The second scenario concerns *realistic sails*. Here, a portion of incoming radiation is reflected, so that ρ is strictly positive and the control set is no more degenerate. In this case, the system is bracket generating. Nevertheless, controllability of the system cannot be assessed because the control set does not contain the origin in its interior (the origin is on the boundary of the control set as depicted in Fig. 1b). Hence, the aforementioned third condition is not satisfied, and the classical approach cannot be used to investigate the controllability of realistic sails.

4 A NECESSARY CONDITION FOR LOCAL CONTROLLABILITY OF SOLAR SAILS

Given some optical properties of the sail and orbital conditions, we are interested in determining if System (3) is small-time locally controllable (STLC). To this purpose, we introduce a necessary condition whose negation guarantees non controllability of the system. Leveraging on the periodic nature of Keplerian motion, the condition states that if there exists a one-form $p_I \in T^*M$, M being the configuration manifold of I, such that

$$\left\langle p_I,\ \frac{\mathrm{d}\, I(f,\boldsymbol{u})}{\mathrm{d}\, t} \right\rangle \geq 0, \qquad \forall\ f \in \mathbb{S}^1,\ \boldsymbol{u} \in \mathcal{U} \tag{4}$$

then there is a half-space of the neighborhood of I where motion is (locally) forbidden and the system is not STLC.

To facilitate the practical evaluation of the necessary condition, two manipulations are introduced. First, the time derivative of I is replaced by $\tilde{G}(I,f)\boldsymbol{u}$, where

$$\tilde{G}(I,f) := (1 + e\cos f) G(I,f) R(I,f)$$

This operation has no impact on the sign of Eq. (4), and it is introduced because $\tilde{G}(I,f)$ is a trigonometric polynomial in f. Such property offers major benefits when positivity constraints are numerically enforced in Section 4.2. We also note that the semi-major axis and planetary constant have no impact on the sign of Eq. (4), so that *all outcomes of the manuscript will be independent of both a and γ_1 (because of symmetry) and valid for any planet since magnitude of SRP does not impact the non-controllability condition*.

Second, control set $\mathcal{U}$ is replaced by its conical hull, $K_\alpha := \mathrm{cone}(\mathcal{U})$, which is a cone of revolution of angle α, as illustrated in Fig. 3. This angle can be deduced from optical properties of the sail. Using Eqs. (1), it is possible to find a relation between cone angle α and specular and diffuse reflectivity coefficients ρ and s respectively. In order to do that, thermal radiation force is neglected, as its magnitude is very small comparing to other forces. The relation is obtained by solving:

$$\tan\alpha = \max_{\beta\in[-\frac{\pi}{2};\frac{\pi}{2}]} \frac{\boldsymbol{f}_{SRP}\cdot\hat{\boldsymbol{s}}}{\left\|\left(\mathbb{I}-\hat{\boldsymbol{s}}\hat{\boldsymbol{s}}^T\right)\boldsymbol{f}_{SRP}\right\|} = \max_{\beta\in[-\frac{\pi}{2};\frac{\pi}{2}]} \frac{\rho\, s\sin 2\beta + B_f\rho(1-s)\sin\beta}{1+\rho\, s\cos 2\beta + B_f\rho(1-s)\cos\beta} \tag{5}$$

This condition holds for:

$$\beta = \cos^{-1}\left(\frac{-B_f\rho(1-s)(3\rho s+1) + \sqrt{B_f^2\rho^2(1-s)^2((3\rho s-1)^2-4\rho s) - 32\rho^2 s^2(\rho s-1)}}{8\rho s}\right)$$

If $B_f = 0$, Eq. (5) simplifies to:

$$\alpha(\rho,s) = \tan^{-1}\left(\frac{\rho\, s}{\sqrt{1-\rho^2\, s^2}}\right), \qquad \rho\, s = \frac{\tan\alpha}{\sqrt{1+\tan^2\alpha}}. \tag{6}$$

Replacing $\mathcal{U}$ by K_α has no impact on the closure of the reachable set of the control system, as discussed in [6]. Therefore, if System (3) is not controllable for controls with values in K_α, then it is not controllable for controls with values in $\mathcal{U}$, neither.

Hence, the necessary condition is recast into:

if $\exists\, p_I \in T^*M$ such that

$$\left\langle p_I,\ \tilde{G}(I,f)\,\boldsymbol{u} \right\rangle \geq 0, \qquad \forall\ f \in \mathbb{S}^1,\ \boldsymbol{u} \in K_\alpha$$

then System (3) is not STLC

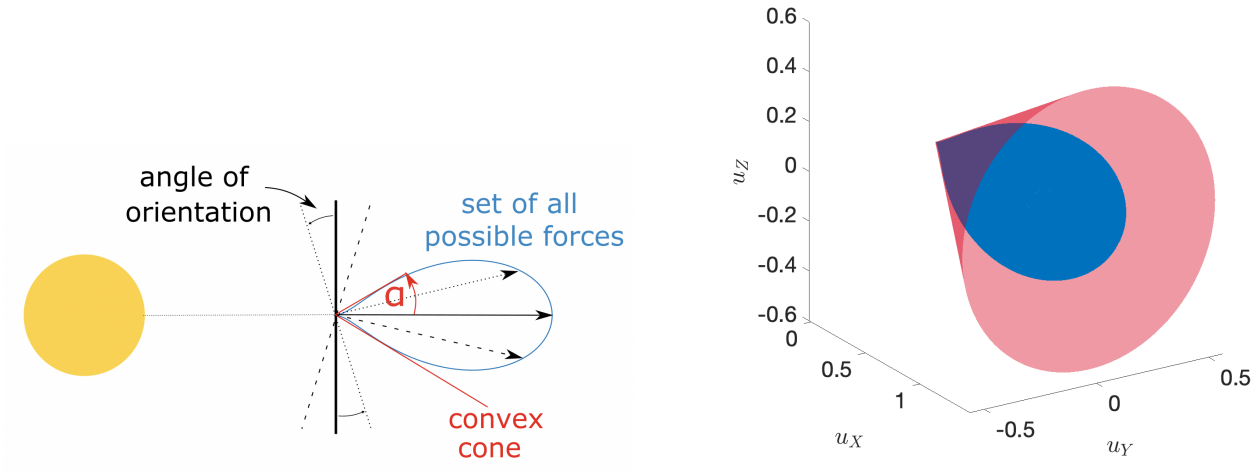

(a) Schematic representation

(b) Three-dimensional representation

Figure 3: Approximation of the control set (blue) by a convex cone (red).

4.1 Constructive approach to verify the necessary condition

A practical check of the necessary condition is carried out by solving

$$\max_{J,\ \|p_I\|\leq 1} J \quad \text{s.t.}$$
$$\left\langle p_I,\ \tilde{G}(I,f)\,\boldsymbol{u} \right\rangle \geq J, \qquad \forall\, f \in \mathbb{S}^1, \quad \forall\, \boldsymbol{u} \in \partial K_\alpha, \|\boldsymbol{u}\| = 1 \tag{7}$$

Problem (7) is convex and semi-infinite, because inequality constraints need to be enforced on two dense sets, namely for all true anomalies between 0 and 2π and for all $\boldsymbol{u}$ on the surface of the cone. Evaluating inequalities in the interior of the cone is not necessary because dynamics is affine in $\boldsymbol{u}$. If J^*, solution of Problem (7), is strictly positive, then the necessary condition is not satisfied and the system is not STLC for the given α and I. Figure 4 illustrates an example of solution of Problem (7) as a function of α. When system is STLC, J^* is zero because $p_I = 0$. The constraint $\|p_I\| \leq 1$ is preferred to $\|p_I\| = 1$ to preserve convexity of Problem (7). Figure 4 shows that a minimum cone angle exists such that the necessary condition is satisfied. This angle can be mapped into minimal requirements for the reflectivity of the sail via Eq. (6), and it can be evaluated by solving

$$\min_{\alpha}\ \alpha \qquad \text{s.t.} \quad J^*(\alpha) = 0 \tag{8}$$

where $J^*(\alpha)$ denotes solution of Problem (7) for a given α.

4.2 Discretization of the optimization problem

Numerical solution of Problem (7) is achieved by:

1. Discretizing K_α by means of a finite number of generators (polyhedral cone);

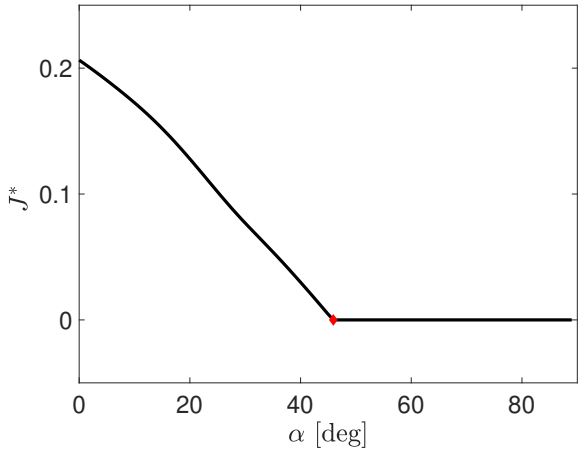

Figure 4: Example of the solution of Problems (7) (black curve) and (8) (red dot). Here, $\gamma_2 = 50$ deg, $\gamma_3 = 40$ deg, and $e = 0.7$.

2. Using the formalism of positive polynomials [7] to enforce positivity constraints for all values of f without introducing additional relaxations.

Let $\boldsymbol{g}_j$, $j = 1, \ldots, m$ be the m generators of the polyhedral cone. Conical combinations can be used to prove that verifying positivity of the inequality constraints for all $\boldsymbol{u} = \boldsymbol{g}_j$, $j = 1, \ldots, m$, namely,

$$p_I^T \tilde{G}(I, f) \boldsymbol{g}_j - J \geq 0 \quad \forall\, f \in \mathbb{S}^1, \quad j = 1, \ldots, m \tag{9}$$

guarantees positivity on the entire surface of the polyhedral cone and its interior. Interior and exterior approximations of the cone can be used, as shown in Fig. 5a. Because we aim at certifying non controllability, we choose exterior approximations. However, results offered in the reminder are obtained by using a large number of generators (namely, $m = 90$) so that differences between the two approximations are deemed negligible, as shown in Fig. 5b for a sample orbit. Convergence depicted in this figure is not monotonic because regular polyhedrals are used, and generators of the m-faced polyhedral do not include the $m - 1$ generators of the preceding approximation.

Inspection of $\tilde{G}(I, f)$ reveals that Eq. (9) is a trigonometric polynomial of degree 2. Let $\langle \cdot, \cdot \rangle_H$ be the Hermitian product of two complex-valued vectors, *i.e.*, $\langle a, b \rangle_H = \langle \mathrm{Re}(a), \mathrm{Re}(b) \rangle + \langle \mathrm{Im}(a), \mathrm{Im}(b) \rangle$, and denote $\Phi(f) = \left[1,\ \mathrm{e}^{if},\ \mathrm{e}^{2if}\right]$ the basis of trigonometric polynomials of degree 2. The left-hand term of Eq.(9) can be reformulated as

$$\left\langle p_I,\ \tilde{G}(I, f)\, \boldsymbol{g}_j \right\rangle - J = p_I^T \left(\sum_{k=-2}^{2} \tilde{G}^{(k)} \mathrm{e}^{i\,k\,f} \right) \boldsymbol{g}_j - J = \left\langle \Phi(f),\ C_j\, p_I - \begin{pmatrix} J \\ 0 \\ 0 \end{pmatrix} \right\rangle_H$$

where $\tilde{G}^{(k)}(I)$ is the k-th coefficient of the Fourier transform of $\tilde{G}(I, f)$, and[2]

$$C_j = \left[\tilde{G}^{(0)} \boldsymbol{g}_j, \quad 2\, \tilde{G}^{(-1)} \boldsymbol{g}_j, \quad 2\, \tilde{G}^{(-2)} \boldsymbol{g}_j \right]^T$$

The formalism of squared functional systems outlined in [7] allows to recast the continuous positivity

[2]We note that $\tilde{G}^k = \overline{\tilde{G}^{(-k)}}$ because $\tilde{G}(I, f)$ is real valued.

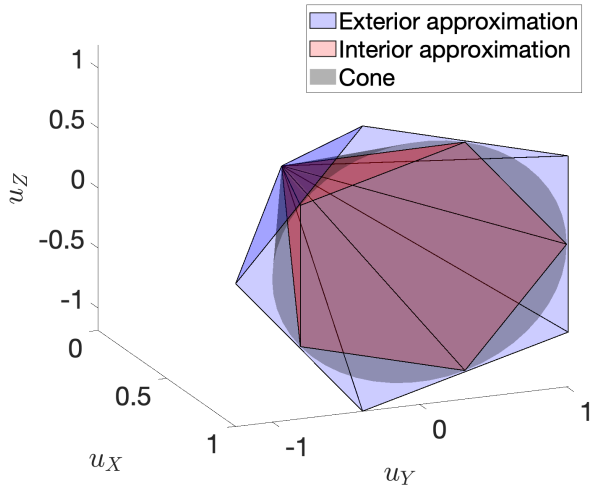

(a) Exterior and interior cone discretization ($m = 5$).

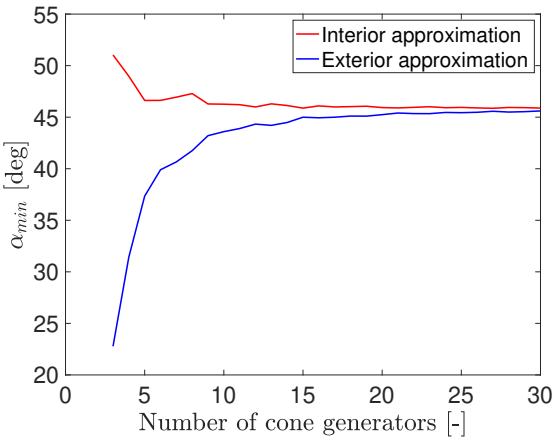

(b) Convergence of the solution of Problem (8) as a function of the number of generators. Here, $\gamma_2 = 50$ deg, $\gamma_3 = 40$ deg, and $e = 0.7$.

Figure 5: Approximation of K_α (grey) by interior and exterior polyhedral cones (red and blue, respectively).

constraints into LMI, namely

$$\left\langle p_I,\ \tilde{G}(I,f)\,\boldsymbol{g}_j \right\rangle - J \geq 0,\ \forall f \in \mathbb{S}^1 \quad \Longleftrightarrow \quad \exists\, Y_j \succeq 0 \ \text{ such that } \ C_j\, p_I - \begin{pmatrix} J \\ 0 \\ 0 \end{pmatrix} = \Lambda_H^*(Y_j)$$

where $\Lambda_H^* : \mathbb{C}^{3\times 3} \to \mathbb{C}^3$ is a linear operator defined in Appendix B, and $Y_j \in \mathbb{C}^{3\times 3}$ are symmetric complex-valued matrices to be determined. Hence, the finite-dimensional counterpart of Problem (7) is

$$\begin{aligned} \min_{J,\, \|p_I\| \leq 1,\, Y_j \in \mathbb{C}^{3\times 3}} \quad & J \quad \text{s.t.:} \\ & Y_j \succeq 0 \\ & \Lambda_H^*(Y_j) = C_j\, p_I - \begin{pmatrix} J \\ 0 \\ 0 \end{pmatrix} \qquad j = 1, \ldots, m \end{aligned} \tag{10}$$

We stress that the only relaxation of Problem (10) with respect to Problem (7) concerns the discretization of the surface of the cone, whereas enforcement of the constraint for all values of f is exact. Finally, solution of Problem (8) is carried out by means of a simple bisection algorithm.

The CVX software [8, 9] is used to solve the convex Problem (10). Fourier coefficients of $\tilde{G}(I, f)$ are evaluated by means of the fast Fourier transform (FFT) algorithm.

5 MINIMAL REQUIREMENTS FOR A SAIL IN PLANET-CENTERED ORBITS

Figure 6 show the minimum cone angle satisfying the necessary condition as a function of γ_2 and γ_3 and with respect to different values of eccentricity. The minimal angle is symmetric with respect to $\gamma_2 = 90$ deg because $\left\langle p_I,\ \tilde{G}(e, \gamma_2, \gamma_3, f)\,\boldsymbol{u} \right\rangle = \left\langle -p_I,\ \tilde{G}(e, \pi - \gamma_2, \gamma_3, f)\,\boldsymbol{u} \right\rangle$. Solution is independent of γ_3 for circular orbits, as expected. Sensitivity with respect to γ_3 remains moderate even for larger eccentricities. The minimal angle approaches zero as $\sin(\gamma_2) \to 0$. In this case, $\hat{\boldsymbol{s}}$ is aligned

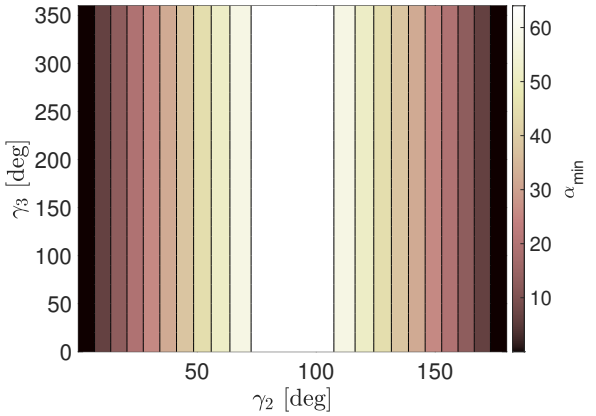

(a) Near-circular orbit: $e \approx 0$

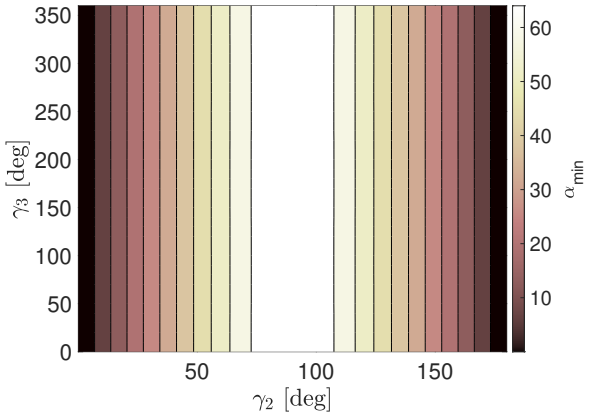

(b) Weak eccentricity $e = 0.1$

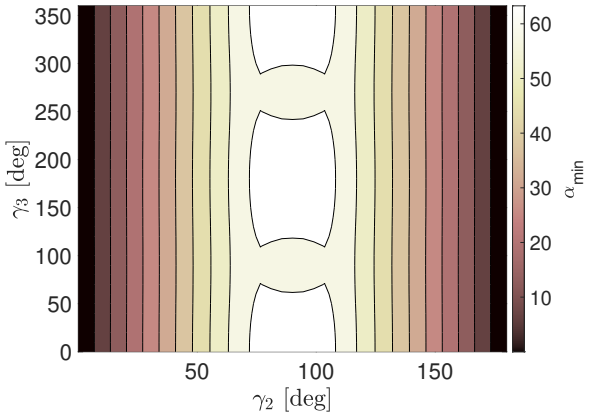

(c) Elliptic orbit with $e = 0.5$

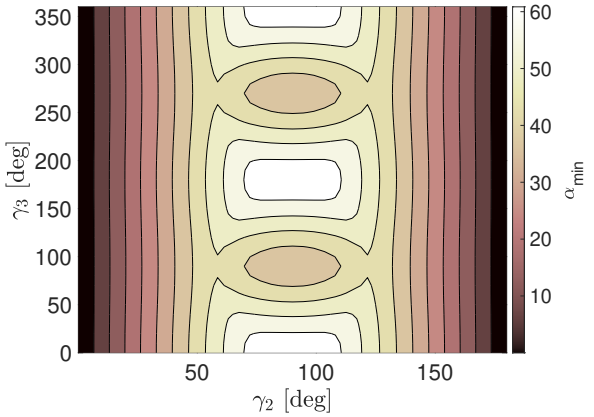

(d) High eccentricity $e = 0.9$

Figure 6: Results for different geocentric orbits

with the angular momentum of the orbit. On the other hand, for $\gamma_2 = 90$ deg, the Sun is in the orbital plane.

Figure 7 represents α_{min} as function of γ_3 or γ_2 (Fig. 7a and 7b, respectively) for different values of eccentricity. Results confirm high dependency of α_{min} on γ_2, and γ_3 for important eccentricity values. Large eccentricity facilitates the controllability of the sail.

Finally, the minimum angle α exists for all orbits, and it is systematically inferior to 90 deg, which means that the sail has not to be ideal to make System (2) controllable. To compare with a real solar sail, optical properties of the NASA reference model [10] (designed to support NEA Scout and Lunar Flashlight solar sail missions) correspond to a cone angle of 58.6 deg. This value is sufficient to satisfy the proposed necessary condition for most planet-centered orbits, except for highly inclined ones.

6 SUN-CENTERED ORBITS

Consider now a sail in a heliocentric orbit. This scenario can be a case for interplanetary transfers, for example. The same equations with two major corrections are used to model the problem. First, the rotation matrix is not needed in Eq. (3) anymore, since the local vertical local horizontal frame is used directly. And second, $\hat{\boldsymbol{s}}$ becomes radial direction. Moreover, the problem has central symmetry and results do not depend on any orbital element except for the eccentricity. For a perfectly absorptive solar sail, the dynamical system is not bracket generating, because the control is radial, as explained

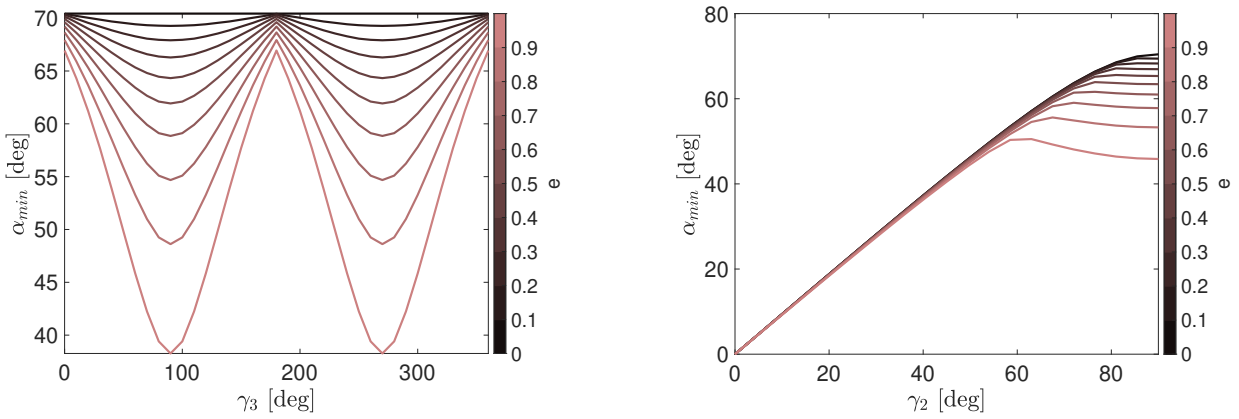

(a) γ_2 fixed at 90 [deg]

(b) γ_3 fixed at 120 [deg]

Figure 7: Minimum cone angle as a function of Euler angles.

in [11]. The first integral related to this rank deficiency is the magnitude of the angular momentum. For a non-ideal sail, the system becomes bracket generating as soon as a tangential component appears: even for very weakly reflective sails.

Using the methodology of Section 4 indicates that even a very poorly reflective sail ($\rho > 0$ and $\rho << 1$) is locally controllable over an orbital period. However, an orbital period around the Sun is much longer compared to a geocentric one, this is why the numerical analysis fails to predict real behaviour of the satellite. In fact, a sail can go in any direction of the tangent manifold of the orbital elements, but the time frame is not considered, so that these maneuvers can take years, which is not realistic. Therefore, a more detailed analysis is needed for heliocentric orbits.

7 CONCLUSION

A necessary condition for local controllability is proposed for solar sails, and it can also be extended to other systems with a control set included in a convex cone. Results show that minimal optical requirements exist for any planet-centered orbit. These requirements only depend on three orbital elements, namely two angles orienting the orbital plane and perigee, and eccentricity. Moreover, they are independent of the planetary constant. The highest minimal angle is strictly inferior to 90 deg, meaning that a certain degree of non-ideality of the sail does not jeopardize controllability of the system. This result can support mission design of solar sails. The methodology was also applied to heliocentric orbits, but a more detailed analysis is needed to account for the non-multi-revolution nature of these trajectories.

A LIE BRACKETS COMPUTATION FOR A PERFECTLY-ABSORPTIVE SAIL

Consider a control-affine dynamical system

$$\dot{x} = F^0(x) + \sum_{i=1}^{m} u_i F^i(x), \quad x \in \mathcal{M}, \quad \boldsymbol{u} = (u_1 ... u_m) \in \mathcal{U} \subset \mathbb{R}^m \tag{11}$$

where $\mathcal{M}$ is an n-dimensional manifold, $F_i : \mathcal{M} \to T\mathcal{M}$ are smooth vector fields on $\mathcal{M}$. We note that Eq. (3) can be recast into the form of Eq. (11) by choosing columns of $G(I, f)R(I, f)$ as vector fields F^i.

To compute Lie algebra, only directions of vector fields matter. To simplify, assume that control system is given by a simple two-body equation with a term of perturbation, as denoted in (12) with $\hat{\boldsymbol{s}}$ solar vector, considered fixed for a few orbits. For a perfectly absorptive solar sail, only the cross-sectional surface is controlled, so that control is assumed to be $u \in [0, 1]$ with a certain coefficient ε defining SRP magnitude.

Using $x = (\boldsymbol{r}, \boldsymbol{v}) \in \mathbb{R}^6$ as a state vector, System (12) can be rewritten as:

$$\dot{x} = F^0(x) + \varepsilon\, u F^1(x)$$

with F^0 recurrent drift and F^1 SRP perturbation.

$$\begin{cases} \dfrac{\mathrm{d}\,\boldsymbol{r}}{\mathrm{d}\,t} = \boldsymbol{v} \\ \dfrac{\mathrm{d}\,\boldsymbol{v}}{\mathrm{d}\,t} = -\dfrac{\mu}{r^3}\boldsymbol{r} + \varepsilon(r_\odot)\,\hat{\boldsymbol{s}} u \end{cases} \tag{12}$$

where $r = \|\boldsymbol{r}\|$. System (12) provides two vector fields:

$$F^0 = v_X \frac{\partial}{\partial r_X} + v_Y \frac{\partial}{\partial r_Y} + v_Z \frac{\partial}{\partial r_Z} - \frac{r_X}{r^3}\frac{\partial}{\partial v_X} - \frac{r_Y}{r^3}\frac{\partial}{\partial v_Y} - \frac{r_Z}{r^3}\frac{\partial}{\partial v_Z}$$
$$F^1 = s_X \frac{\partial}{\partial v_X} + s_Y \frac{\partial}{\partial v_Y} + s_Z \frac{\partial}{\partial v_Z}$$

To simplify, let us denote vector fields:

$$v\frac{\partial}{\partial r} = v_X \frac{\partial}{\partial r_X} + v_Y \frac{\partial}{\partial r_Y} + v_Z \frac{\partial}{\partial r_Z}, \quad \frac{r}{r^3}\frac{\partial}{\partial v} = \frac{r_X}{r^3}\frac{\partial}{\partial v_X} + \frac{r_Y}{r^3}\frac{\partial}{\partial v_Y} + \frac{r_Z}{r^3}\frac{\partial}{\partial v_Z}$$
$$s\frac{\partial}{\partial v} = s_X \frac{\partial}{\partial v_X} + s_Y \frac{\partial}{\partial v_Y} + s_Z \frac{\partial}{\partial v_Z}$$

and

$$F^{sr} = s\frac{\partial}{\partial r},\ F^{rr} = r\frac{\partial}{\partial r},\ F^{vr} = v\frac{\partial}{\partial r},\ F^{sv} = s\frac{\partial}{\partial v},\ \ldots$$

Finally, by denoting $\hat{\boldsymbol{s}} \cdot \boldsymbol{r}$ a scalar product of two vectors $\hat{\boldsymbol{s}}$ and $\boldsymbol{r}$, computation of Lie brackets gives the following results:

$$F^0 = v\frac{\partial}{\partial r} - \frac{r}{r^3}\frac{\partial}{\partial v} = F^{vr} - \frac{1}{r^3}F^{rv}; \quad F^1 = s\frac{\partial}{\partial v} = F^{sv}; \quad F^{01} = \Big[F^0, F^1\Big] = -F^{sr}$$
$$F^{001} = \Big[F^0, [F^0, F^1]\Big] = \frac{3\,(\hat{\boldsymbol{s}} \cdot \boldsymbol{r})}{r^5}\,F^{rv} - \frac{F^{sv}}{r^3}, \quad F^{101} = \Big[F^1, [F^0, F^1]\Big] = 0$$
$$F^{0001} = \Big[F^0, [F^0, [F^0, F^1]]\Big] = \frac{1}{r^3}F^{sr} + \frac{3(\boldsymbol{v} \cdot \boldsymbol{r})}{r^5}F^{sv} + \Big(\frac{3(\hat{\boldsymbol{s}} \cdot \boldsymbol{v})}{r^5} - \frac{15(\hat{\boldsymbol{s}} \cdot \boldsymbol{r})(\boldsymbol{v} \cdot \boldsymbol{r})}{r^7}\Big)F^{rv}$$
$$+ \frac{3(\hat{\boldsymbol{s}} \cdot \boldsymbol{r})}{r^5}(F^{vv} - F^{rr})$$

All subsequent iterations are linear combinations of the previous vector fields. Thus, Lie algebra of the system (12) has 5 independent vector fields if $\hat{\boldsymbol{s}} \cdot \boldsymbol{r} \neq 0$:

$$F^{sr},\ F^{sv},\ F^{rv},\ F^{vr},\ F^{vv} - F^{rr}\,.$$

$$\dim \mathrm{Lie}(F^0, F^1, ...) = 5 \quad < \quad \dim \mathbb{R}^6 = 6$$

B POSITIVE POLYNOMIALS

Consider the basis of trigonometric polynomials $\Phi = \left(1, e^{if}, e^{2if}, \ldots, e^{N_{\text{freq}}if}\right)$ with N_{freq} number of frequencies. Its corresponding squared functional system is $\mathcal{S}^2(f) = \Phi(f)\Phi^H(f)$ where $\mathcal{S}^H(f)$ denotes conjugate transpose of $\mathcal{S}(f)$. Let $\Lambda_H : \mathbb{C}^N \to \mathbb{C}^{N\times N}$ be a linear operator mapping coefficients of polynomials in $\Phi(f)$ to the squared base, so that application of Λ_H on $\Phi(f)$ yields

$$\Lambda_H(\Phi(f)) = \Phi(f)\Phi^H(f)$$

and define its adjoint operator $\Lambda_H^* : \mathbb{C}^{N\times N} \to \mathbb{C}^N$ as

$$\langle Y, \Lambda_H(c)\rangle_H \equiv \langle \Lambda_H^*(Y), c\rangle_H, \quad Y \in \mathbb{C}^{N\times N}, \quad c \in \mathbb{C}^N.$$

Theory of squared functional systems postulated by Nesterov [7] proves that polynomial $\left\langle \Phi(f), c\right\rangle_H$ is non-negative for all $f \in \mathbb{S}^1$ if and only if a Hermitian positive semidefinite matrix Y exists such that $c = \Lambda_H^*(Y)$, namely

$$\langle \Phi(f), c\rangle_H \geq 0, \ \forall f \in \mathbb{S}^1 \quad \Longleftrightarrow \quad \exists Y \succeq 0 : c = \Lambda_H^*(Y).$$

In fact in this case it holds

$$\begin{aligned}\left\langle \Phi(f), c\right\rangle_H &= \left\langle \Phi(f), \Lambda_H^*(Y)\right\rangle_H = \left\langle \Lambda_H(\Phi(f)), Y\right\rangle_H, \\ &= \left\langle \Phi(f)\Phi^H(f), Y\right\rangle_H = \Phi^H(f)\, Y\, \Phi(f) \geq 0.\end{aligned}$$

For trigonometric polynomials Λ^* is given by

$$\Lambda^*(Y) = \begin{bmatrix} \langle Y, T_0\rangle \\ \vdots \\ \langle Y, T_{N-1}\rangle \end{bmatrix}$$

where T_j $j = 0, \ldots, N-1$ are Toeplitz matrices such that

$$T_0 = I, \ \ T_j^{(k,l)} = \begin{cases} 2 & \text{if } k - l = j \\ 0 & \text{otherwise} \end{cases} \quad j = 1, \ldots, N-1$$

REFERENCES

[1] C. R. McInnes, *Solar Sailing*. London: Springer London, 1999. [Online]. Available: http://link.springer.com/10.1007/978-1-4471-3992-8

[2] L. Rios-Reyes and D. J. Scheeres, "Generalized model for solar sails," *Journal of Spacecraft and Rockets*, vol. 42, no. 1, pp. 182–185, jan 2005. [Online]. Available: https://doi.org/10.2514%2F1.9054

[3] B. Dachwald, M. Macdonald, C. R. McInnes, G. Mengali, and A. A. Quarta, "Impact of Optical Degradation on Solar Sail Mission Performance," *Journal of Spacecraft and Rockets*, vol. 44, no. 4, pp. 740–749, Jul. 2007. [Online]. Available: https://arc.aiaa.org/doi/10.2514/1.21432

[4] O. Montenbruck and E. Gill, *Satellite Orbits*. Springer Science + Business Media, 2000. [Online]. Available: http://dx.doi.org/10.1007/978-3-642-58351-3

[5] V. Jurdjevic, *Geometric Control Theory*, 1st ed. Cambridge University Press, 1996. [Online]. Available: https://www.cambridge.org/core/product/identifier/9780511530036/type/book

[6] A. Herasimenka, J.-B. Caillau, L. Dell'Elce, and J.-B. Pomet, "Control of a Solar Sail: An augmented version of "Effective Controllability Test for Fast Oscillating Control Systems. Application to Solar Sailing"," Apr. 2021, working paper or preprint. [Online]. Available: https://hal.inria.fr/hal-03185532

[7] Y. Nesterov, "Squared Functional Systems and Optimization Problems," in *High Performance Optimization*, P. M. Pardalos, D. Hearn, H. Frenk, K. Roos, T. Terlaky, and S. Zhang, Eds. Boston, MA: Springer US, 2000, vol. 33, pp. 405–440, series Title: Applied Optimization. [Online]. Available: http://link.springer.com/10.1007/978-1-4757-3216-0_17

[8] M. Grant and S. Boyd, "CVX: Matlab software for disciplined convex programming, version 2.1," http://cvxr.com/cvx, Mar. 2014.

[9] ——, "Graph implementations for nonsmooth convex programs," in *Recent Advances in Learning and Control*, ser. Lecture Notes in Control and Information Sciences, V. Blondel, S. Boyd, and H. Kimura, Eds. Springer-Verlag Limited, 2008, pp. 95–110, http://stanford.edu/~boyd/graph_dcp.html.

[10] A. F. Heaton and A. Artusio-Glimpse, "An update to the NASA reference solar sail thrust model," in *AIAA SPACE 2015 Conference and Exposition*. American Institute of Aeronautics and Astronautics, aug 2015. [Online]. Available: https://doi.org/10.2514%2F6.2015-4506

[11] B. Bonnard, , J.-B. Caillau, E. Trélat, and and, "Geometric optimal control of elliptic keplerian orbits," *Discrete & Continuous Dynamical Systems - B*, vol. 5, no. 4, pp. 929–956, 2005. [Online]. Available: https://doi.org/10.3934%2Fdcdsb.2005.5.929